

Longitudinal motion control of electric vehicles: Glocal model and design using passivity

Binh-Minh Nguyen¹, João Pedro F. Trovão², Minh C. Ta², and Michihiro Kawanishi¹
¹Toyota Technological Institute, ²University of Sherbrooke

This article presents a framework to model and design the longitudinal motion control system for electric vehicles (EVs). Thanks to the passivity property of EV, a hierarchical control configuration including three layers is proposed. In the lower layer, each actuator is provided a disturbance observer (DOB) for locally preventing the wheel slip. A global controller is designed in the upper layer for the cruising purpose. Besides, the middle layer serves as the aggregation and distribution channels. The conditions for the controllers to sufficiently guarantee L_2 stability of the system, even when the aggregation/distribution ratios are time-varying, are presented. This allows the realization of additional global objectives, such as energy optimization problems. Moreover, L_2 stability conditions can be verified conveniently without the need of establishing the dynamical equations of the overall system. The simplicity and efficacy of the proposed framework are discussed through several examples with test results.

Motion control of EV: Issues remain unsolved

Motion control of electric vehicles (EVs) has emerged as an active research field during the last two decades thanks to the advantages of electric motors [1]. This article deals with a related sub-field, namely, longitudinal motion control (LMC).

Through a literature review, LMC can be organized into three main groups. The first one is wheel slip ratio control; the slip ratio can be managed by a PI controller [1] or a sliding mode controller [2]. The next group is anti-slip control; anti-slip can be realized by several methods such as disturbance observer (DOB) based control [1], [3], maximum transmissible torque estimation [4], and wheel speed control [5]. The last group is driving force control that is based on driving force observer [6].

Despite the great successes that have already been achieved, several issues still needed to be resolved. The first issue is from a theoretical point of view. Due to the characteristics of tire-friction force [7], an EV is fundamentally nonlinear. Also, the road conditions frequently change during real-time operations. Therefore, stabilization of LMC system is a theoretical challenge. For instance, [1] and [3] used a traditional DOB design tool that treated the originally nonlinear EV as a nominal linear plant with norm-bounded perturbation for robust stability analysis. As pointed out in [8], this does not rigorously show system stability.

Moreover, EVs also belong to the class of multi-actuator systems (Fig. 1). However, almost all of the previous studies in LMC neglected the physical interaction between the local actuators. As shown in [9], even if each wheel's speed control



Figure 1 Multi-motor EVs: a four-wheel EV driven by in-wheel-motors and a three-wheel EV with in-wheel-motors in the front.

loop is stabilized by pole placement, this does not automatically guarantee the stability of the LMC system as a whole. This is due to the fact that the performance of the overall system should be determined by both the local subsystem's transfer function and a matrix that represents physical interaction [10]. Due to the change of operating points, the poles of the overall system might move toward the imaginary axis with increasing imaginary parts. This might degrade the performance of slip ratio control by introducing the fluctuation phenomenon [10]. To deal with physical interactions, we have utilized two approaches, namely "generalized frequency variables" in [9] and "hierarchically decentralized LQR" in [10]. However, [9] and [10] require non-trivial calculations, such as linearization about an operating point and Riccati equation solving in real-time.

Last but not least, we should maintain the EV's safe motion and simultaneously minimize its energy consumption. Although some coordinated frameworks have been proposed, they merely considered upper-layer motion control, such as yaw-rate control [11], [12] and vehicle speed control [13]. A typical example is range extension control [13], which was based on speed control without anti-slip. As discussed later, a small slip ratio is necessary to reduce energy consumption.

Proposed framework

The goal of this article is twofold. First, with respect to the nonlinearity of vehicle dynamics and the physical interaction between motor actuators, it aims to develop practical-oriented procedure to design and stabilize LMC system with less computational burden. Second, it aims to integrate global energy management with slip prevention at local actuators.

To achieve its goals, this article was motivated by passivity theory, which was initially introduced to robotics [14]. The robot arm is actually a complex system with nonlinearities and uncertainties. Fortunately, it belongs to the class of systems that do not produce internal energy, or *passive* systems. Hence, L_2 stability of the robot system can be assured in a convenient way. We only need to establish the feedback connection of the robot with a passive controller. After three decades, passivity has been successfully applied to various applications, such as power systems, DC-DC converters, and motor drives [15]. It would be a pity if the passivity theory had been neglected in the research field of EVs. This article proposes a passivity-based framework to model and design LMC systems for EVs.

By proving the passivity property of EV, this article presents a hierarchical control configuration in Fig. 2. To deal with the current challenges of DOB [8], this article intentionally utilized it for the lower-layer. For cruise control, a global controller is designed in the upper-layer. The middle-layer serves as the aggregation and distribution channels. Depending on the switch SW and the flag FL, the system has three motion control modes as the following:

Mode 1 (SW = 0, FL = 1): human driving with anti-slip.

Mode 2 (SW = 1, FL = 0): cruise control.

Mode 3 (SW = 1, FL = 1): fully-functional mode.

Road condition is identifiable by using electric motor torques and on-board sensors [1]. If the system detects that the vehicle enters the low friction surface, then Modes 1 and 3 must be used. The driving mode with (SW = 0, FL = 0) is acceptable if the vehicle operates on the high friction surface.

The key idea of this article is to use the torque distribution vector to aggregate the motor speeds. This configuration ensures a passivity property of the single-input single-output subsystem which includes the middle-layer, EV and the lower-layer controller. Interestingly, the passivity property of the aforementioned subsystem is maintained even with time-varying distribution ratios. This allows for an energy management strategy by performing an optimization problem on the set of distribution ratios. Moreover, each control layer can be designed independently without establishing the dynamical equation of the overall system. Consequently, the complexity of system design can be reduced as linearization process is no longer required. Based on passivity theory, this article obtains the condition that sufficiently guarantees L_2 stability of the control system in Modes 1, 2, and 3.

Global model of EV longitudinal dynamics

In Fig. 2, block EV describes the dynamical model of the M -wheel vehicle in which each wheel is driven by an electric motor. The reader can find the definitions of all physical parameters and motion variables in Table 1 of the Appendix.

The EV can be seen as the feedback connection of the global dynamics \mathbf{G} with M local dynamics \mathbf{L}_i . \mathbf{G} describes the longitudinal motion of the vehicle; its input is the aggregation of all driving forces, and its output is the longitudinal speed. Each \mathbf{L}_i describes the local rotational motion of the motor, gear and wheel mechanism with the equivalent moment of inertia $J_{eq,i}$. It has two inputs and two outputs. The input of vehicle speed is distributed from the upper-layer; and the motor torque $T_{m,i}$ is the local control signal. The driving force F_i is aggregated to the global dynamics; and the motor speed can be utilized for the motion control purposes. The map $f(\cdot)$ from slip ratio to driving force is described by "magic formula" [7].

Passivity analysis

Definition of passivity

Definition 1 [16]: We consider a dynamical system H with the input u and the output y in the Euclidean p -space, and the state x in the Euclidean n -space. H is said to be passive if there exists a positive semidefinite function S defined from Euclidean n -space to the non-negative real number space, called storage function, such that the time derivative of S is no more than the inner product of y and u . In addition, H is input strictly passive (ISP) or output strictly passive (OSP) if

$$\dot{S} \leq y^\dagger u - \delta_u \|u\|^2 \quad \text{or} \quad \dot{S} \leq y^\dagger u - \delta_y \|y\|^2 \quad (1)$$

holds for some positive numbers δ_u or δ_y .

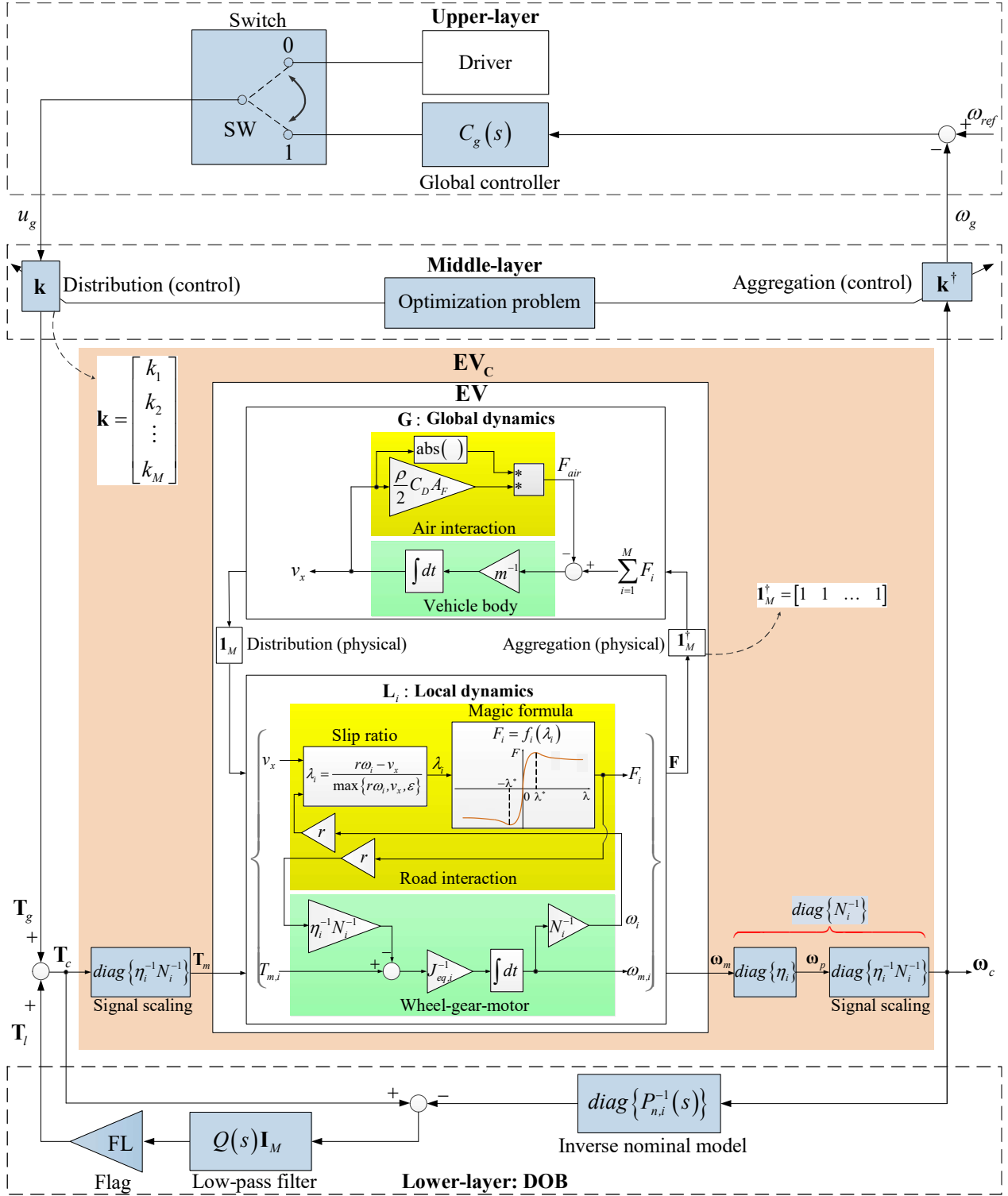


Figure 2 Glocal model and the glocal control system for the EV driven by M motor actuators.

Notice: (i) In-wheel-motor EV can also be modelled by setting the gear ratio N_i and the gear efficiency η_i to be one. (ii) The gravity does not appear. It is treated as disturbance, and can be compensated by feedback controller. (iii) \mathbf{I}_M is the identity matrix of size M . (iv) The vehicle is modelled by block EV with motor torque vector \mathbf{T}_m as the input, and motor speed vector ω_m as the output. (v) In the slip ratio formula, ε is a small positive number to avoid division by zero. (vi) The physical interaction between the motor actuators is represented by the distribution and aggregation vector $\mathbf{1}_M$.

Passivity of EV

Proposition 2: The EV is passive from the motor torque \mathbf{T}_m to the scaled speed ω_p with the energy storage function

$$S = \frac{1}{2} m v_x^2 + \frac{1}{2} \sum_{i=1}^M \eta_i J_{eq,i} \omega_{m,i}^2 \quad (2)$$

Proof: Based on the dynamics of \mathbf{G} and \mathbf{L}_i shown in Fig. 2, we can obtain

$$\begin{aligned} \omega_p^\dagger \mathbf{T}_m - \dot{S} &= \sum_{i=1}^M \eta_i \omega_{m,i} T_{m,i} - m \dot{v}_x v_x - \sum_{i=1}^M \eta_i J_{eq,i} \dot{\omega}_{m,i} \omega_{m,i} \\ &= \frac{1}{2} \rho C_D A_F v_x^2 |v_x| + \sum_{i=1}^M \lambda_i f_i(\lambda_i) \max\{r\omega_i, v_x, \varepsilon\} \end{aligned} \quad (3)$$

We notice that the term $\lambda_i f_i(\lambda_i)$ is non-negative for any value of the slip ratio. Consequently, the right-hand side of (3) is the summation of all non-negative terms. Following **Definition 1**, the EV is shown to be passive.

There exists another way to prove the passivity of the EV. It is to use the “divide to conquer” approach. The readers are invited to show that the subsystems \mathbf{G} and \mathbf{L}_i are also passive. Then, the EV is shown to be passive since it is actually the feedback connection of passive subsystems [16].

Glocal control design

Preliminary discussion

As shown in Fig. 2, the extended vehicle model EV_C is established by a pair of pre-and-post scaling matrices. The output of EV_C , or ω_c , has the meaning of the wheel speed vector. Thus, it can be used for motion control purposes. With respect to the scaling matrices, EV_C is also passive from \mathbf{T}_c to ω_c . This passivity notation allows many ways to design LMC systems. The straightforward idea is to connect between the output and the input of EV_C a strictly passive controller.

Notice: As can be seen from [5], it is possible to estimate the slip ratio at each local wheel using the motor torque and motor speed. Using the estimated slip ratios, we can introduce another scaling matrix after ω_c to obtain an estimated speed of the vehicle body.

Design procedure

The stability of the system in Fig. 2 can be discussed from its equivalent diagram in Fig. 3, in which $C_{eqg}(s)$ and $C_{eqi}(s)$ are the equivalent transfer functions. The design procedure consists of three stages as the following:

Stage 1 (Lower-layer): Select for each actuator a nominal model $P_{n,i}(s)$, and select a low-pass filter $Q(s)$ such that the transfer function $1/(1-Q(s))$ is stable and $C_{eqi}(s)$ is ISP.

Stage 2 (Middle-layer): Depending on the design purpose, solve an optimization problem to obtain a distribution vector \mathbf{k} which is non-zero and norm-bounded.

Stage 3 (Upper-layer): Select an OSP global controller $C_g(s)$ such that $C_{eqg}(s)$ is also OSP.

Stability analysis

Proposition 3: The proposed glocal design procedure sufficiently ensures that the glocal control system has a finite L2-gain in either Mode 1, Mode 2 or Mode 3.

Proof: First, in Mode 1 with $\{\text{SW} = 0, \text{FL} = 1\}$, the system becomes the feedback connection of the passive system EV_C and $\text{diag}\{C_{eqi}\}$. If each C_{eqi} is ISP, it can be show by **Definition 1** that the aforementioned system (in the red-dashed rectangle) is OSP from \mathbf{T}_{eqg} to ω_c . The fundamental passivity theorem [16] shows that the system has a finite L2-gain.

Next, Mode 2 is examined. Since $\text{FL} = 0$ and $\text{SW} = 1$, the system becomes the feedback connection of EV_C and C_g via the aggregation and distribution vectors. We have $\mathbf{T}_c = \mathbf{T}_{eqg}$ and

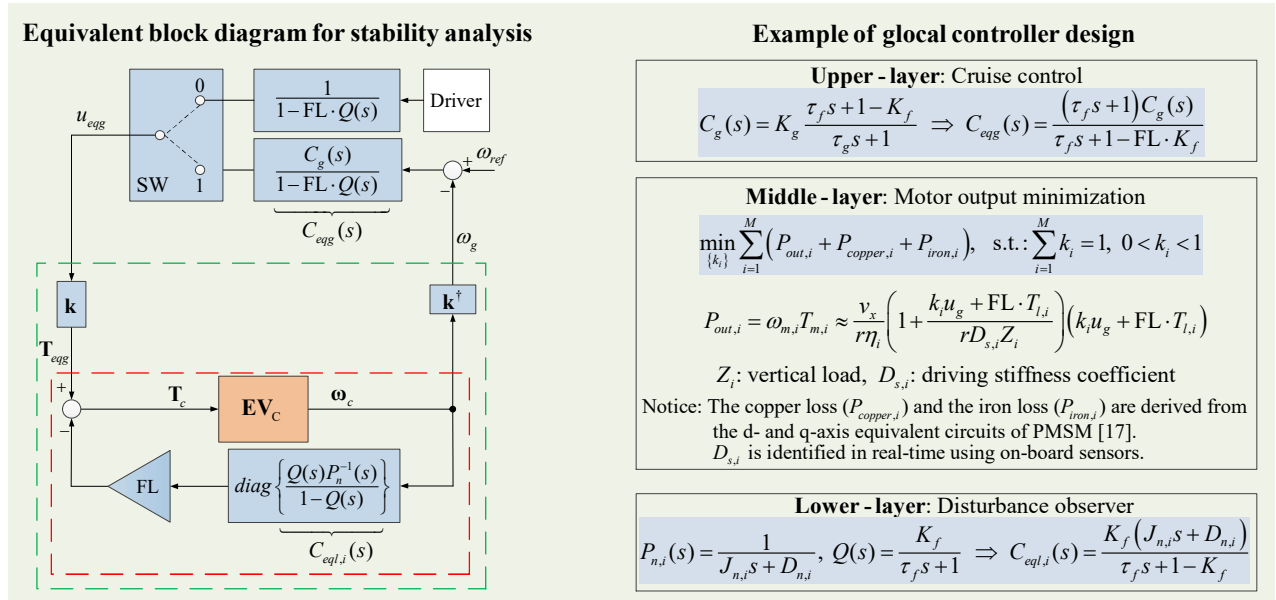


Figure 3 Equivalent expression of the control system, and a design example.

$$0 \leq \omega_c^\dagger \mathbf{T}_c - \dot{S} = \omega_c^\dagger (u_{eqg} \mathbf{k}) - \dot{S} = \omega_g u_{eqg} - \dot{S} \quad (4)$$

The above inequality holds true even when the distribution ratios are time-varying. Thus, the lower-layer system in the green-dashed rectangle is passive from u_{eqg} to ω_g . If C_g is OSP, then the system in Mode 2 is OSP from ω_{ref} to u_{eqg} . Thus, the system has a finite L₂-gain and is L₂ stable in this mode.

Finally, Mode 3 with {SW = 1, FL = 1} is investigated. If $C_{eq,i}$ is ISP, then the system in the red-dashed rectangle is OSP from \mathbf{T}_{eqg} to ω_c . Applying Cauchy-Schwarz inequality, the lower-layer system in the green-dashed rectangle is OSP from u_{eqg} to ω_g . Again, this OSP property holds true even when the distribution ratios are time-varying. If C_{eqg} is OSP, then the overall system is the feedback connection of two OSP systems. According to the fundamental passivity theorem [16], the overall system has a finite L₂-gain and is L₂ stable in Mode 3.

Design example

Considering the EV driven by permanent magnet synchronous motors (PMSMs), a candidate of the control system design is summarized in Fig. 3.

Lower layer: The DOB was designed with the nominal model parameters $J_{n,i}$ and $D_{n,i}$. Besides, the low-pass filter was selected with the time constant τ_f and K_f is a tuning gain which should be between 0 and 1.

Middle layer: To improve the energy management for EV, it is possible to minimize the summation of motor output power $\{P_{out,i}\}$ with the copper loss $\{P_{copper,i}\}$ and the iron loss $\{P_{iron,i}\}$.

The driving force is linearized as $F_i = D_{s,i} Z_i \lambda_i$ where $D_{s,i}$ is the driving stiffness coefficient and Z_i is the vertical load of the wheel [10], [13]. Both $D_{s,i}$ and Z_i can be estimated in real-time using on-board sensors. Based on the EV dynamics in Fig. 2, the motor output power $P_{out,i}$ can be approximated as a quadratic function of the distribution ratio k_i .

$P_{copper,i}$ and $P_{iron,i}$ can be formulated using motor's equivalent circuit studied by Morimoto *et al* [17]. We assumed that the d -axis currents of the motors are maintained at zero. Under this assumption, the copper loss and iron loss can be represented as quadratic functions of the distribution ratio k_i .

In summary, the summation P_{in} of all $\{P_{out,i}\}$, $\{P_{copper,i}\}$ and $\{P_{iron,i}\}$ can be expressed as a quadratic function of $\{k_i\}$. This allows the optimization problem to be solved in real-time without special difficulty.

Upper-layer: The global controller C_g was selected as a compensator.

Notice: In the real EV, the motor torque is limited by the maximum motor current. Besides, the current control loop has a certain bandwidth. Therefore, the global control gain K_g must have its maximum value $K_{g,max}$ which can be found by fine-tuning process. If K_g is bigger than $K_{g,max}$, the system will suffer vibration of motor torque. Similarly, there exists the maximum value $K_{f,max}$ for the DOB's tuning gain. If K_f is close to 0, the DOB is almost eliminated. If K_f is close to $K_{f,max}$, the DOB operates with maximum performance. However, this

might degrade the acceleration of the vehicle and result in the uncomfortable feeling of the driver. This trade-off should be compromised by the designer.

Remark

Remark 1: The traditional way of controller design is to establish the dynamic equation of the overall system. Unfortunately, this centralized way is quite complex for the EV system which includes nonlinearities and uncertainties. The passivity notation provides us a practical way. In other words, each control layer can be designed separately. It is only required to check the passivity properties of a transfer function $C_{eqg}(s)$ and M transfer functions $\{C_{eq,i}(s)\}$. The designer might represent a given transfer function in state space and then applying **Definition 1** to check its passivity. Another way is to use the Kalman-Yakubovich-Popov (KYP) Lemma [15] to amount the passivity condition to linear matrix inequality (LMI) which can be solved using several programming languages as Matlab, Python, and C/C++.

Remark 2: If the saturation of motor torque should be addressed, then EV_c could not be treated as passive system. Fortunately, the torque saturation operator and the slip ratio-driving force map can be lumped into an equivalent map with sector bounded nonlinearity. This allows absolute stability analysis by applying Circle & Popov criterion [16].

Remark 3: The proposed framework is not limited to driving torque distribution. Using the motor loss model [17], P_{in} can be derived as a convex function of $\{k_i\}$ and the d -axis currents $\{I_{d,i}\}$ of the motors. Energy management can be further improved by optimizing the allocation of motor torques and motor currents simultaneously.

Remark 4: By introducing additional constraints to $\{k_i\}$, it is also possible to generate the yaw, roll, or pitch moments. This means the proposed LMC can be easily integrated with other sub-fields of EV motion control, such as lateral stability control, roll stability control, and pitch stability control.

Remark 5: If a linearized model of EV is available, we might define some control performances using infinity norm. For instance, the local performance is to match the transfer function of the local subsystem with a nominal shared model. Another local performance is to minimize the infinity norm of the transfer function from the disturbance to the wheel speed. Besides, the global performance is to track the aggregated speed with the reference speed. Given a volume of the shared model set, a robust control tool (i.e., μ -synthesis) can be utilized to optimize the controllers [18].

Application 1: 4-wheel-EV

Description of the vehicle

The relationship between anti-slip performance and energy consumption reduction was demonstrated by the 4-wheel blue EV shown in Fig. 1. The rear wheels of the vehicle are driven

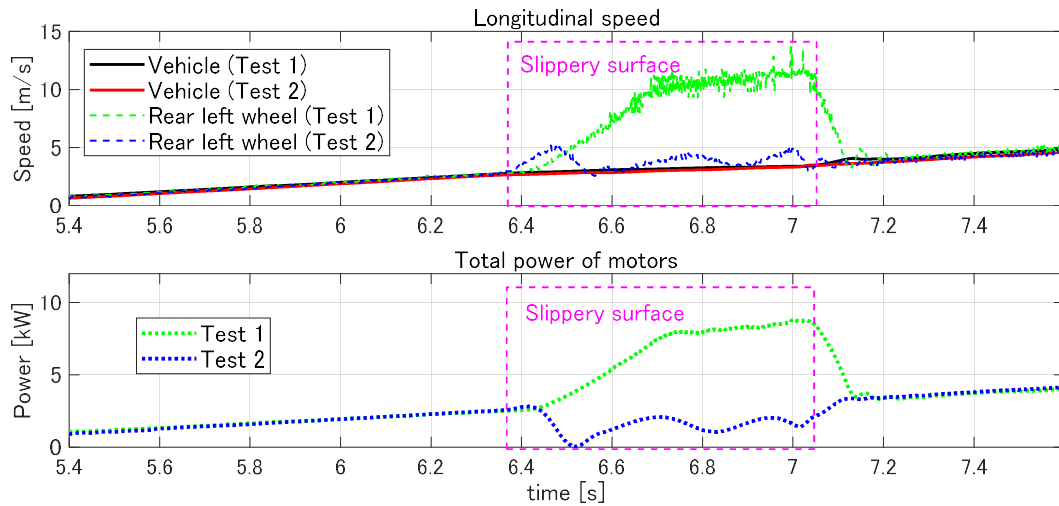


Figure 4 Experimental results of the four-wheel EV driven by in-wheel-motors.

by in-wheel-motors of PMSM type. A detailed explanation of the vehicle system was presented in [10]. Several key parameters of the vehicle were presented in Table 1 of the Appendix.

Motion control can improve energy management

This example is to show that motion control can improve the way of using energy for EVs. To this end, two test cases were conducted as follows.

Test 1: The system operates in human driving mode without DOB. In other words, the driving torque commands of the motors are always maintained constantly.

Test 2: Mode 1 will be turned-on if the system detects a sharp decreasing in the driving stiffness value which can be estimated using motor torque and on-board sensors [6], [10].

The torque commands of the motors will be adjusted by DOB.

A plate made from polymer material was covered with water to create the slippery surface with low friction coefficient (Fig. 1). In both test cases, the driver gave the driving command of 200 [N.m] which was equally distributed to the rear-left and rear-right wheels. To clearly observe the test results, we only plotted in Fig. 4 the speeds of the vehicle and the rear-left wheel. In contrast to Test 1, Test 2 shows that the vehicle only experienced a small wheel slip when entering the slippery surface. Thus, Test 2 is much safer than Test 1 from a motion control point of view. According to **Proposition 2**, the increasing of motor speed in Test 1 will result in an increasing of motor power on the slippery surface. Consequently, to operate the vehicle with the same speed pattern, Test 1 required more energy than that of Test 2.

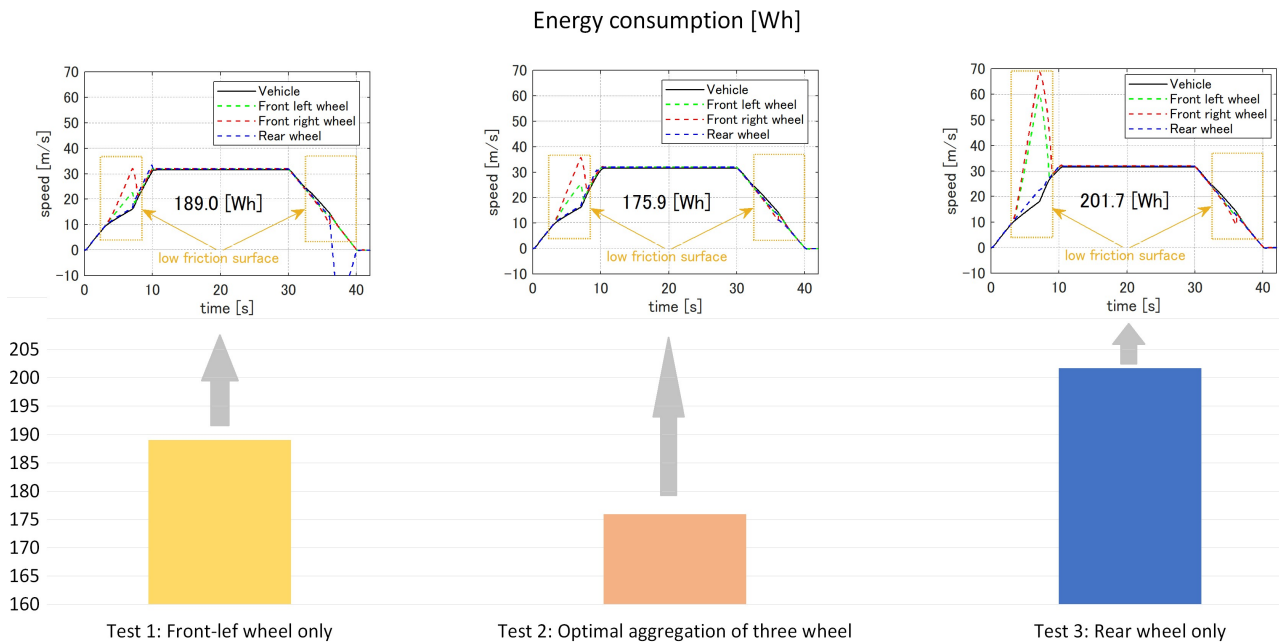


Figure 5 Test results of the three-wheel EV using Mode 2 with different speed aggregation strategies.

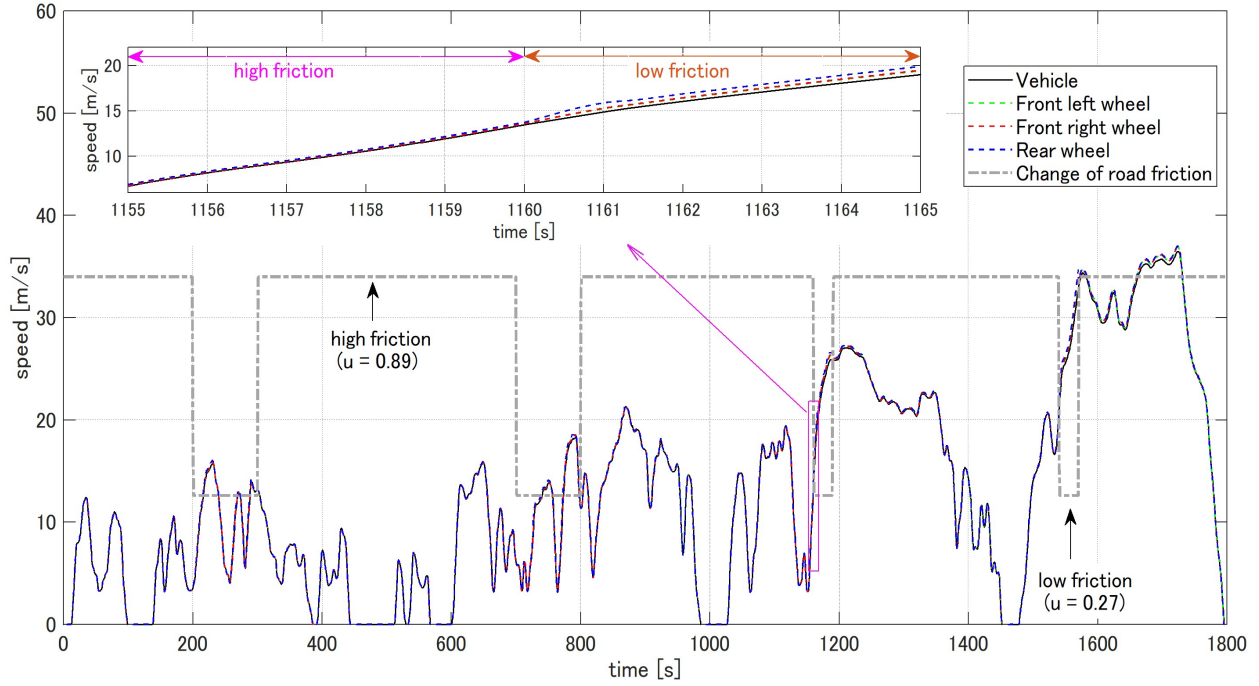


Figure 6 WLTC test: speed pattern and the friction coefficient of the road surface.

Application 2: 3-wheel recreational EV

Description of the vehicle

First, this Section is to show the merit of the hierarchical control configuration with aggregation and distribution. Second, it demonstrates the effectiveness of the proposed framework using a standard driving test. To this end, this study used the 3-wheel-EV prototype shown in Fig. 1. This prototype has been used as a workbench for research in our group [19]. The new vehicle is now driven by a 13kW permanent magnet synchronous motor (PMSM) connected to the rear wheel through two pulleys and a belt. Besides, two 4kW PMSMs are directly connected to the front wheels. The main physical parameters of the 3-wheel EV are also presented in Table 1 of the Appendix.

Description of the control system

Lower-layer: The filter $Q(s)$ was selected with the time constant $\tau_f = 0.05$ and $K_f = 0.70$. Considering the motor inertia, the wheel inertia, and the static load of each wheel, the nominal models were selected with $J_{n,1} = J_{n,2} = 10.70$, $J_{n,3} = 13.68$ and $D_{n,1} = D_{n,2} = 0.10$, $D_{n,3} = 0.15$.

Middle-layer: Assuming that the road conditions of the front left and front right wheels are almost similar, we set the distribution ratios of the front wheels as $k_1 = k_2 = k_f$, and the distribution ratio of the rear wheel is $k_3 = 1 - 2k_f$. The optimization problem becomes finding the gain k_f that minimizes the summation of motor input powers. This problem can be solved by a standard Lagrange multiplier algorithm.

Upper-layer: By fine-tuning process, the global controller was selected with $\tau_g = 0.10$ and $K_g = 1200.00$.

By using Matlab, $C_{eq,i}(s)$ and $C_{eq}(s)$ are shown to be not only OSP but also ISP. Following **Proposition 3**, the above selection of the controller is ready for evaluation.

Merit of the proposed aggregation/distribution

To clarify the merit of the proposed control configuration, we conducted the following test using Mode 2 (without DOB). The vehicle accelerated to 114 [km/s] or 31.7 [m/s] in 10 seconds. It maintained this speed constantly until 30 seconds, and finally decelerated to stop at 40 seconds. From 3 to 7 seconds, and from 32 seconds until the end of the test, the vehicle had to run on the low friction surface ($\mu = 0.27$). Three cases were examined. They had the same torque distribution strategy which minimized the motor input power. However, they used different speed aggregation strategies. In Tests 1 and 3, we only sent to the upper-layer the speed of the front-left motor and rear motor, respectively. In Test 2, we used the proposed approach which aggregates the speeds of all motors.

As can be seen from Fig. 5, the wheel slip was prevented to a certain extent in Test 2. In contrast, Tests 1 and 3 suffered from wheel slip in the deceleration and acceleration periods, respectively. Consequently, Test 2 could reduce the energy consumption in comparison with Tests 1 and 3. In summary, the proposed control architecture can improve not only the safety but also the energy performance of the vehicle. The idea of improvement is to maintain an equality between the actuators. If a motor was allocated more torque, then it should contribute more to the aggregated speed.

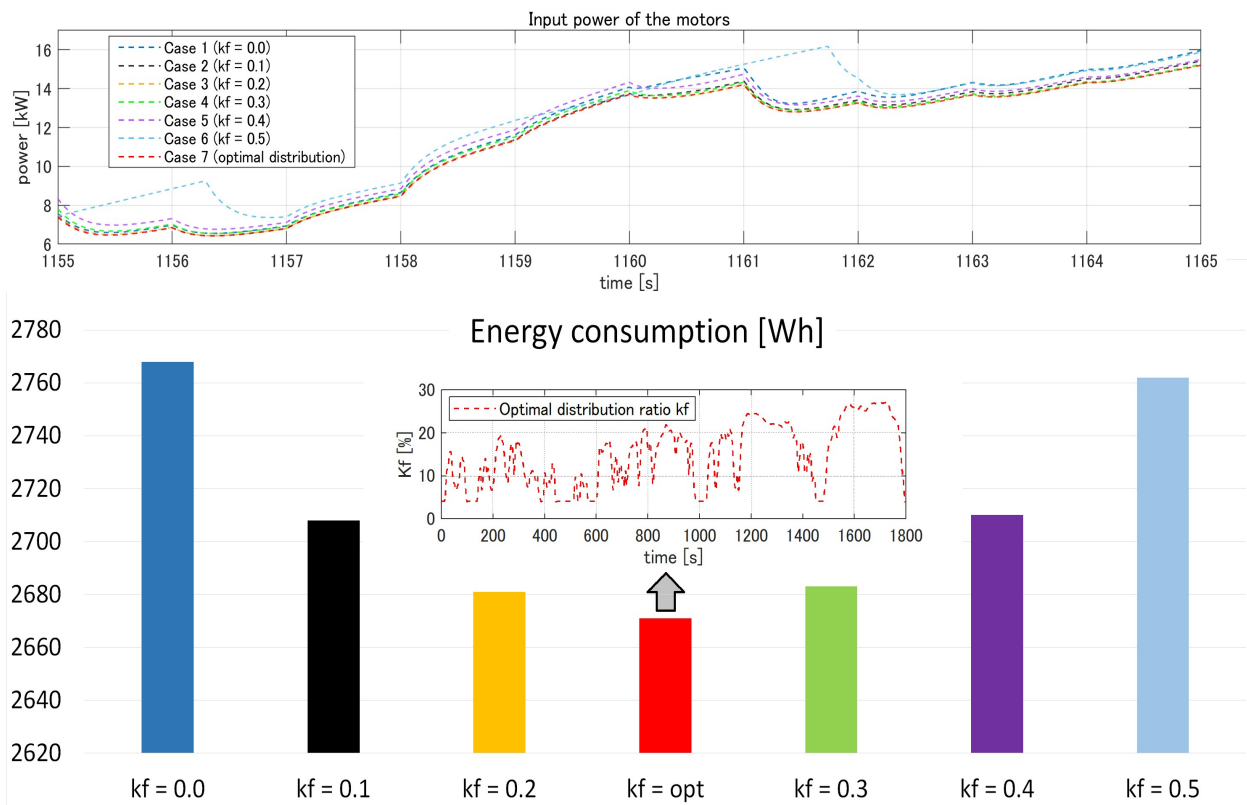


Figure 7 Results of WLTC tests using the e-TESC recreational EV prototype.

WLTC test

The performance of the proposed control system was evaluated by the worldwide harmonized light-duty vehicle test cycles (WLTC) (Fig. 6). Mode 2 was used during four sections with high friction road surface ($\mu = 0.89$). Mode 3 was turned on during four sections with low friction ($\mu = 0.27$). Seven distribution strategies were performed for comparisons. The distribution ratio k_f was fixed to 0.0, 0.1, 0.2, 0.3, 0.4, 0.5 from Case 1 to Case 6. In Case 7, k_f was optimally updated at every 1 millisecond. Thanks to the proposed control system, safe motion of the vehicle was attained. Actually, the wheel speeds and the vehicle speeds were almost the same for all test cases. As a representative, Fig. 6 only demonstrated the vehicle speed and wheel speeds of Case 7. As can be seen from Fig. 7, more energy was saved by Case 7 with the optimal distribution strategy. On the other hand, Case 1 (rear-wheel driving) and Case 6 (front-driving) were quite extreme from an energy point of view.

Fig. 7 also shows the total input power of all motors between 1155 [s] and 1165 [s]. This is one of the most critical periods as the vehicle entered the low friction surface with high acceleration and high speed. Even though, we did not observe any sharp increase in motor power. Moreover, the total motor power was minimized by the optimal distribution strategy.

In summary, the WLTC test showed that an energy related issue could be realized in the proposed global framework.

Conclusion: Bring energy back to EV

Tolstoy said: “All happy families [linear systems] are alike, every unhappy family [nonlinear one] is unhappy [nonlinear] in its own way” [15]. Fortunately, EV shares the same fundamental property with robots, RLC circuits, and many other nonlinear systems in the real world: the passivity. This allows us to develop a “divide to conquer approach” to model, analyze, and design global motion control of EV.

The merits of the passivity based global framework are twofold. From theoretical point of view, L_2 stability of the system can be shown rigorously without complex mathematic calculations. From practical point of view, the global and local objectives are attained by a simple design procedure. Passivity is shown to be a convenient framework to deal with energy optimization problems. A new vision of motion control and energy management can be hence opened. Moreover, the passivity notation can be utilized to develop networked control for EVs. In a narrow scenario with a single EV, we might realize wireless control of motor actuators. In a broader scenario with EV platoon, we might integrate platoon consensus control with energy management.

The effectiveness of the passivity framework has been discussed through a design example which was applied to an in-wheel-EV and a recreational EV prototype. It can straightforwardly be extended to other motion control goals, such as slip ratio control and driving force control. It can also

be extended to other EV prototypes, such as hybrid EV which includes both electric motors and internal combustion engines. Also, its architecture can easily consider other control issues, such as robust control performance and adaptive control as well as intelligent energy management.

Appendix

The physical parameters, the motion variables, and the parameters of two vehicles used for evaluation are summarized in Table 1.

Acknowledgements

This work was supported in part by Grant 950-230672 from Canada Research Chairs Program, and in part by Grant 2019-NC-252886 from *Fonds de recherche du Québec – Nature et Technologies*.

The concept of “glocal (global/local) control” has been proposed by Prof. Shinji Hara (Tokyo Institute of Technology, Japan). We would like to thank him for giving us a motivation to pursue the framework presented in this article.

Finally, we would like to thank Prof. Yoichi Hori (the University of Tokyo, Japan) for the great support of research motivations and experimental environment.

References

- [1] Y. Hori, “Future Vehicle Driven by Electricity and Control-Research on 4 Wheel Motored UOT Mach II,” *IEEE Transactions on Industrial Electronics*, Vol. 51, No. 5, pp. 954-962, 2004.
- [2] D. Savitski, V. Ivanov, K. Augsburg, T. Emmei, H. Fuse, H. Fujimoto, and L. M. Fridman, “Wheel Slip Control for the Electric Vehicle with In-Wheel Motors: Variable Structure and Sliding Mode Methods,” *IEEE Transactions on Industrial Electronics*, Vol. 67, pp. 8535-8544, 2020.
- [3] L. Li, S. Kodama, and Y. Hori, “Design of Anti-Slip Controller for an Electric Vehicle with an Adhesion Status Analyzer Based on the EV Simulator,” *Asian Journal of Control*, Vol. 8, No. 3, pp. 261-267, 2006.
- [4] D. Yin, S. Oh, and Y. Hori, “A Novel Traction Control for EV Based on Maximum Transmissible Torque Estimation,” *IEEE Transactions on Industrial Electronics*, Vol. 56, No. 6, pp. 2086-2094, 2009.
- [5] T. Suzuki and H. Fujimoto, “Slip Ratio Estimation and Regenerative Brake Control without Detection of Vehicle Velocity and Acceleration for Electric Vehicle at Urgent Brake-turning,” *Proceedings of the 11th IEEE International Workshop on Advanced Motion Control*, pp. 273-278, 2010.
- [6] K. Maeda, H. Fujimoto, and Y. Hori, “Four-wheel Driving-force Distribution Method for Instantaneous or Split Slippery Roads for Electric Vehicle,” *Automatika*, Vol. 54, No. 1, pp. 103-113, 2013.
- [7] H. B. Pacejka, “Tyre and Vehicle Dynamics,” Elsevier BV, 2006.
- [8] E. Sariyildiz, R. Oboe, and K. Ohnishi: “Disturbance Observer-Based Robust Control and Its Applications: 35th Anniversary Overview,” *IEEE Transaction on Industrial Electronics*, Vol. 67, Iss. 3, pp. 2042-2053, 2020.
- [9] B-M. Nguyen, H. V. Nguyen, M. Ta-Cao, and M. Kawanishi, “Longitudinal Modelling and Control of In-Wheel-Motor Electric Vehicles as Multi-Agent Systems,” *Energies*, 13, 5437, 2020.

Symbol	Definition
i	Index of the local actuator (i from 1 to M)
\dagger	Transpose notation of vector and matrix
Vehicle body	
m	Vehicle mass
h_{cg}	Height of the center of gravity (CoG)
l_f, l_r	Distances from front (rear) axles to the CoG
A_F	Frontal area of vehicle in the air
C_d	Drag coefficient
ρ	Air density
v_x	Longitudinal speed of the vehicle
Wheel	
$J_{w,i}$	Moment of inertia of the wheel
r	Radius of the wheel
ω_i	Rotational speed of the wheel
Motor	
$J_{m,i}$	Moment of inertia of the motor
$\omega_{m,i}$	Rotational speed of the motor
$T_{m,i}$	Motor torque
Gear	
N_i	The i th gear ratio
η_i	The i th gear efficiency
Wheel-Gear-Motor system	
$J_{eq,i}$	Equivalent moment of inertia of wheel-gear-motor
Slip ratio and tire force	
λ_i	Slip ratio of the i th wheel.
ε	A small positive number to avoid division-by-zero
F_i	Driving force of the i th wheel.
Z_i	Vertical force at the i th wheel
Definition of the signals in the glocal control system	
ω_{ref}	Reference speed
ω_g	Aggregated speed of all wheels
u_g	Global control signal (output of the upper-layer)
Vectors of size M	Control signals from middle-layer and lower-layer T_g : vector of $\{T_{g,i}\}$, T_r : vector of $\{T_{r,i}\}$
	Torque and rotational speed of motor T_m : vector of $\{T_{m,i}\}$, ω_m : vector of $\{\omega_{m,i}\}$
	Torque and speed of the extended model EV _C T_c : vector of $\{T_{c,i}\}$, ω_c : vector of $\{\omega_{c,i}\}$
	Scaled speed for passivity analysis ω_p : vector of $\{\omega_{p,i}\}$
Parameters of the vehicles used in experiment/simulation	
4-wheel EV	Vehicle body $m = 400$ [kg], $h_{cg} = 0.3$ [m], $l_f = 0.8$ [m], $l_r = 0.4$ [m]
	Wheel $J_{w,i} = 1.26$ [kg.m ²], $r = 0.3$ [m]
3-wheel EV	Vehicle body $m = 370$ [kg], $C_D = 0.75$, $A_F = 1.25$ [m ²], $h_{cg} = 0.7$ [m], $l_f = 0.678$ [m], $l_r = 1.039$ [m]
	Wheel $J_{w,1,2} = 0.68$ [kg.m ²], $J_{w,3} = 1.06$ [kg.m ²], $r = 0.27$ [m]
	Motor $J_{m,1,2} = 0.060$ [kg.m ²], $J_{m,3} = 0.096$ [kg.m ²]
	Gear $N_{1,2} = 1$, $N_3 = 5.033$, $\eta_{1,2} = 1$, $\eta_3 = 0.95$

Table 1 List of nomenclatures and vehicle parameters.

- [10] B-M. Nguyen, S. Hara, H. Fujimoto, and Y. Hori, "Slip Control for IWM Vehicles Based on Hierarchical LQR," *Control Engineering Practice*, Vol. 93, 104179, 2019.
- [11] Y. Suzuki, Y. Kano, and M. Abe, "A Study on Tyre Force Distribution Controls for Full Drive-by-wire Electric Vehicle," *Vehicle System Dynamics*, Vol. 52, pp. 235-250, 2014.
- [12] C. Chatzikomis, M. Zanchetta, P. Gruber, A. Sorniotti, B. Modic, T. Motaln, L. Blagotinsek, and G. Gotovac, "An Energy-efficient Torque-vectoring Algorithm for Electric Vehicles with Multiple Motors," *Mechanical Systems and Signal Processing*, Vol. 8, pp. 655-673, 2019.
- [13] Y. Ikezawa, H. Fujimoto, Y. Hori, D. Kawano, Y. Goto, M. Tsuchimoto, and K. Sato, "Range Extension Autonomous Driving for Electric Vehicles Based on Optimal Velocity Trajectory Generation and Front-Rear Driving-Braking Force Distribution," *IEEJ Journal of Industry Application*, Vol. 5, No. 3, pp. 228-235, 2016.
- [14] R. Ortega and M. W. Spong, "Adaptive Control of Robot Manipulators: A Tutorial," *Automatica*, Vol. 25, No. 6, pp. 877-888, 1989.
- [15] R. Ortega, J. A. Loria Perez, P. J. Nicklasson, and H. Sira-Ramirez, "Passivity-based Control of Euler-Lagrange Systems," Springer, 1998.
- [16] H. K. Khalil, "Nonlinear Systems," Prentice Hall, 2002.
- [17] S. Morimoto, Y. Tong, Y. Takeda, and T. Hirasa, "Loss Minimization Control of Permanent Magnet Synchronous Motor Drives," *IEEE Transactions on Industrial Electronics*, Vol. 41, No. 5, pp. 511-517, 1994.
- [18] S. Hara, K. Tsumura, and B-M. Nguyen, "Hierarchically Decentralized Control for Networked Dynamical Systems with Global and Local Objectives," *Emerging Applications of Control and System Theory*, Springer, 2017.
- [19] J. P. Trovao, M-A. Roux, E. Menard, and M. R. Dubois, "Energy and Power-Split Management of Dual Energy Storage System for a Three-Wheel Electric Vehicle," *IEEE Transactions on Vehicular Technology*, Vol. 66, Iss. 7, pp. 5540-5550, 2016.

Binh-Minh Nguyen (binhminh@toyota-ti.ac.jp) was a researcher at the Department of Information Physics and Computing, the University of Tokyo, Tokyo, Japan. He is currently a researcher at Toyota Technological Institute, Aichi, Japan. His main research interests include global control, robust control, and their applications to electric vehicles, flying vehicles, and power systems.

João Pedro F. Trovão (Joao.Trovao@USherbrooke.ca) is a Professor with the Department of Electrical Engineering and Computer Engineering, University of Sherbrooke, Sherbrooke, QC, Canada, where he holds the Canadian Research Chair position in Efficient Electric Vehicles with Hybridized Energy Storage Systems and the Founding (E) Director of the electric-Transport, Energy Storage and Conversion (e-TESSC) Lab. His main research interests cover the areas of electric vehicles, hybridized energy storage systems, energy management and rotating electrical machines.

Minh C. Ta (Cao.Minh.Ta@USherbrooke.ca) was with Hanoi University of Science and Technology, Vietnam, where he became an Associate Professor in 2009 and was the Founding Director of the Center for Technology Innovation (2009-2018). He is currently an Associate Professor with the Department of Electrical and Computer Engineering, University of Sherbrooke, Sherbrooke, QC, Canada. His main research interests include motor drives and advanced control techniques and their applications to electric vehicles and energy conversion systems.

Michihiro Kawanishi (kawa@toyota-ti.ac.jp) was a Research Associate at Kobe University, Kobe, Japan, from 1996 to 2006. In 2006 he became an Associate Professor at Toyota Technological Institute, Aichi, Japan. His main research interests include control system design with numerical optimization and its application to mechanical systems.